How to cite: *Angew. Chem. Int. Ed.* **2022,** *61,* e202202492
International Edition: doi.org/10.1002/anie.202202492
German Edition: doi.org/10.1002/ange.202202492

2D COFs

# Combination of Knoevenagel Polycondensation and Water-Assisted Dynamic Michael-Addition-Elimination for the Synthesis of Vinylene-Linked 2D Covalent Organic Frameworks

*Shunqi Xu, Zhongquan Liao, Arezoo Dianat, Sang-Wook Park, Matthew A. Addicoat, Yubin Fu, Dominik L. Pastoetter, Filippo Giovanni Fabozzi, Yannan Liu, Gianaurelio Cuniberti, Marcus Richter, Stefan Hecht, and Xinliang Feng**

**Abstract:** Vinylene-linked two-dimensional conjugated covalent organic frameworks (V-2D-COFs), belonging to the class of two-dimensional conjugated polymers, have attracted increasing attention due to their extended π-conjugation over the 2D backbones associated with high chemical stability. The Knoevenagel polycondensation has been demonstrated as a robust synthetic method to provide cyano (CN)-substituted V-2D-COFs with unique optoelectronic, magnetic, and redox properties. Despite the successful synthesis, it remains elusive for the relevant polymerization mechanism, which leads to relatively low crystallinity and poor reproducibility. In this work, we demonstrate the novel synthesis of CN-substituted V-2D-COFs via the combination of Knoevenagel polycondensation and water-assisted dynamic Michael-addition-elimination, abbreviated as **KMAE** polymerization. The existence of C=C bond exchange between two diphenylacrylonitriles (**M1** and **M6**) is firstly confirmed via in situ high-temperature NMR spectroscopy study of model reactions. Notably, the intermediate **M4** synthesized via Michael-addition can proceed the Michael-elimination quantitatively, leading to an efficient C=C bond exchange, unambiguously confirming the dynamic nature of Michael-addition-elimination. Furthermore, the addition of water can significantly promote the reaction rate of Michael-addition-elimination for highly efficient C=C bond exchange within 5 mins. As a result, the **KMAE** polymerization provides a highly efficient strategy for the synthesis of CN-substituted V-2D-COFs with high crystallinity, as demonstrated by four examples of V-2D-COF-TFPB-PDAN, V-2D-COF-TFPT-PDAN, V-2D-COF-TFPB-BDAN, and V-2D-COF-HATN-BDAN, based on the simulated and experimental powder X-ray diffraction (PXRD) patterns as well as $N_2$-adsorption–desorption measurements. Moreover, high-resolution transmission electron microscopy (HR-TEM) analysis shows crystalline domain sizes ranging from 20 to 100 nm for the newly synthesized V-2D-COFs.

## Introduction

Two-dimensional π-conjugated covalent organic frameworks (2D c-COFs), which belong to the class of crystalline 2D conjugated polymers with in-plane π-conjugation and regular 2D framework structures, are attractive materials for potential applications in optoelectronics, spintronics, photocatalysis, and energy storage.[1–11] For the solution synthesis of 2D c-COFs, dynamic covalent chemistry, which can form-break-reform covalent bonds under a dynamic equilibrium (error-correction process), is indispensable for forming thermodynamically controlled crystalline frameworks.[5,9] So

[*] Dr. S. Xu, Dr. S.-W. Park, Dr. Y. Fu, D. L. Pastoetter, Dr. Y. Liu, Dr. M. Richter, Prof. X. Feng
Chair of Molecular Functional Materials, Center for Advancing Electronics Dresden (cfaed) and Faculty of Chemistry and Food Chemistry, Technische Universität Dresden,
Mommsenstrasse 4, 01069 Dresden (Germany)
E-mail: xinliang.feng@tu-dresden.de

Dr. S. Xu, Prof. X. Feng
Department of Synthetic Materials and Functional Devices, Max-Planck Institute of Microstructure Physics,
06120 Halle (Germany)

Dr. Z. Liao
Fraunhofer Institute for Ceramic Technologies and Systems (IKTS)
01109 Dresden (Germany)

Dr. A. Dianat, Prof. G. Cuniberti
Chair of Material Science and Nanotechnology, Faculty of Mechanical Science and Engineering, Technische Universität Dresden,
Hallwachstraße 3, 01069 Dresden (Germany)

Dr. M. A. Addicoat
School of Science and Technology, Nottingham Trent University,
Clifton Lane, Nottingham, NG11 8NS (UK)

F. G. Fabozzi, Prof. S. Hecht
DWI-Leibniz Institute for Interactive Materials & Institute of Technical and Macromolecular Chemistry,
RWTH Aachen University,
52074 Aachen (Germany)

Dr. S.-W. Park
Leibniz-Institute for Polymer Research Dresden e.V. (IPF)
01069 Dresden (Germany)

© 2022 The Authors. Angewandte Chemie International Edition published by Wiley-VCH GmbH. This is an open access article under the terms of the Creative Commons Attribution Non-Commercial NoDerivs License, which permits use and distribution in any medium, provided the original work is properly cited, the use is non-commercial and no modifications or adaptations are made.


© 2022 The Authors. Angewandte Chemie International Edition published by Wiley-VCH GmbH

far, the most reported 2D c-COFs are limited to the imine-linked[4,7,12–14] and triazine-linked 2D c-COFs.[15–17] However, due to the high polarization of C=N bond, imine- and triazine-linked 2D c-COFs exhibit a moderate electron delocalization with poor conjugation.[6,18–21] Moreover, the imine-linked 2D c-COFs generally suffer from poor chemical stability, which hinders their potential for robust applications.[22,23]

Vinylene-linked 2D covalent organic frameworks (V-2D-COFs, or vinylene-linked 2D conjugated polymers) have recently attracted arising attention because of the robust and superb π-conjugated framework structures with high chemical stability.[24–29] Several synthetic methodologies, including Knoevenagel-,[24,25] other Aldol-type-,[29–32] and Horner–Wadsworth–Emmons[19] based 2D polycondensation approaches, have been developed. Particularly, several CN-substituted V-2D-COFs have been successfully synthesized via Knoevenagel polycondensation, and demonstrated superior performance as magnetic materials,[25] organic cathodes for lithium-ion batteries,[23] luminescence,[33–35] and photocatalysis,[20,36–38] compared with their corresponding imine-linked 2D COF analogs. Nevertheless, the mechanism understanding for the formation of crystalline CN-substituted V-2D-COFs remains elusive. It is still challenging to control the reversibility of the Knoevenagel 2D polycondensation, which is essential to enhance the crystallinity and reproducibility for the synthesis of V-2D-COFs.[39,40] Therefore, it is highly desirable to achieve a deep insight into the polymerization mechanism, including the driving force for the error-correction process and controlled reaction conditions for synthesizing highly crystalline CN-substituted V-2D-COFs.

In this work, we report a novel and highly reproducible strategy—the combination of Knoevenagel polymerization and water-assisted dynamic Michael-addition-elimination (classified as **KMAE** polymerization)—for the synthesis of highly crystalline CN-substituted V-2D-COFs (Figure 1a). A dynamic C=C bond exchange of model reaction of diphenylacrylonitrile (**M1**) and (4-methylphenyl)-acetonitrile (**M3**) toward (*Z*)-3-phenyl-2-(*p*-tolyl)acrylonitrile (**M6**) and benzonitrile (**M2**) is firstly demonstrated via in situ high-temperature (HT) NMR investigations (Figure 1b). In particular, the intermediate 2,3,4-triphenylpentanedinitrile (**M4**, R=H) as the product of the Michael-addition of **M1** and **M2** (R=H) can proceed the Michael-elimination with a high yield up to ≈95 %, strongly suggesting the Michael-addition-elimination as a dynamic chemistry for the C=C bond exchange. Significantly, HT NMR measurements reveal that the addition of water can significantly facilitate the Michael-addition-elimination for the C=C bond exchange, reaching equilibrium with a ratio of 1:1 for **M1** (**M3**) and **M6** (**M2**) within 5 min. Thereby, the combination

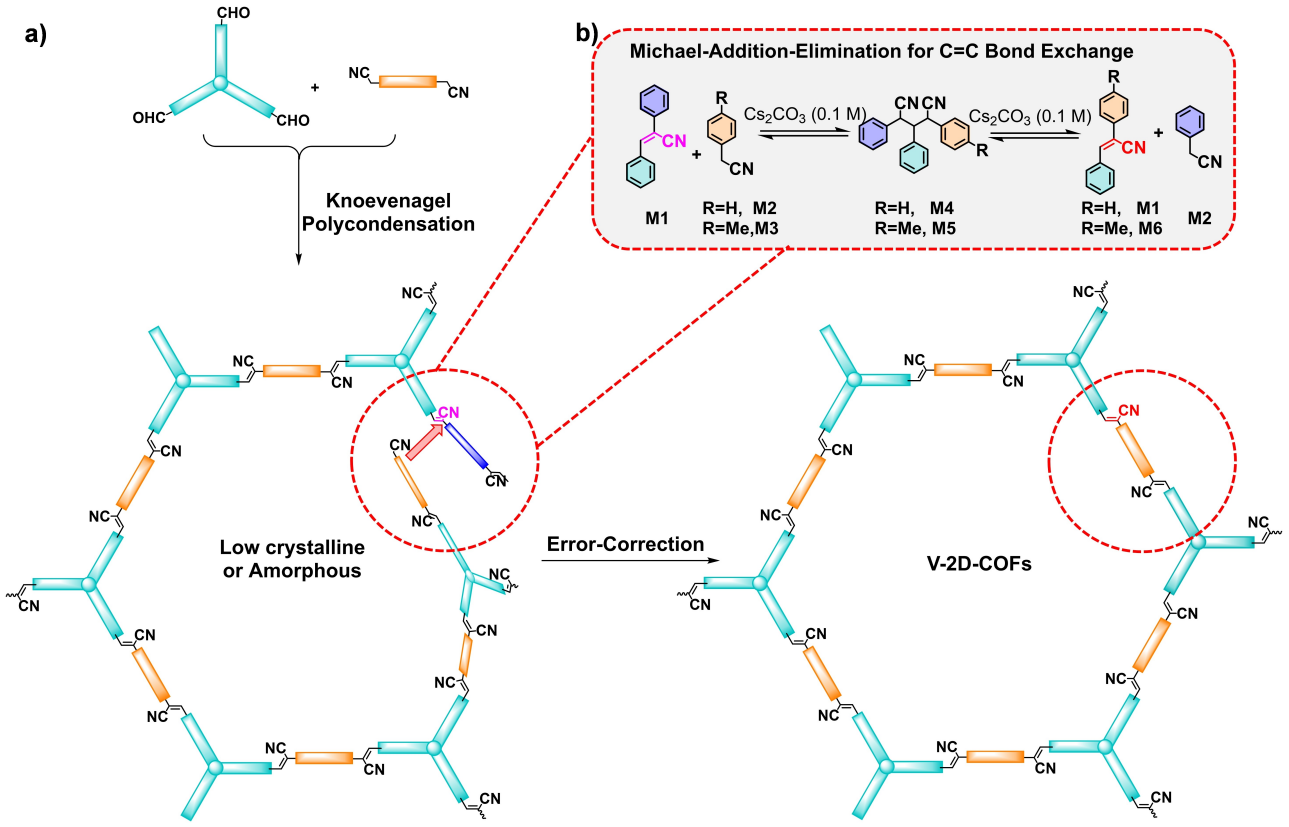


***Figure 1.*** a) The synthesis of CN-substituted V-2D-COFs via the Knoevenagel and in situ Michael-Addition-Elimination polymerization (KMAE polymerization). b) The dynamic Michael-addition-elimination for the C=C bond exchange is confirmed by the efficient conversion of diphenylacrylonitrile (**M1**) and (4-methylphenyl)-acetonitrile (**M3**) to (*Z*)-3-phenyl-2-(*p*-tolyl)acrylonitrile (**M6**) and phenylacetonitrile (**M2**).


© 2022 The Authors. Angewandte Chemie International Edition published by Wiley-VCH GmbH

of Knoevenagel polycondensation and water-assisted Michael-addition-elimination (**KMAE** polymerization) is demonstrated as a highly efficient and reproducible strategy for the synthesis of highly crystalline CN-substituted V-2D-COFs. Four examples, including V-2D-COF-TFPB-PDAN (V-2D-COF-1, also abbreviated as 2D PPV in literature),[24] V-2D-COF-TFPT-PDAN (V-2D-COF-2), V-2D-COF-TFPB-BDAN (V-2D-COF-3), and V-2D-COF-HATN-BDAN (V-2D-COF-4) are demonstrated by using the **KMAE** polymerization. According to simulated and experimental PXRD patterns and $N_2$-adsorption-desorption measurements with matched pore-size distributions, highly crystalline CN-substituted V-2D-COFs can be synthesized via $A_3B_2$ and $A_6B_2$ polymerization from various monomers, including $C_3$-symmetric 1,3,5-tris-(4-formylphenyl)benzene (TFPB), (2,4,6-tris(4-formylphenyl)-1,3,5-triazine (TFPT), 2,3,8,9,14,15-hexa(4-formylphenyl)diquinoxalino[2,3-a:2′,3′-c]phenazine (HATN-6CHO), and $C_2$-symmetric (1,4-phenylene)diacetonitrile (PDAN), and 2,2′-(biphenyl-4,4′-diyl)diacetonitrile (BDAN). Moreover, high-resolution transmission electron microscopy (HR-TEM) analysis exhibits crystalline domains with the range of 20–100 nm for V-2D-COF-1, V-2D-COF-3, and V-2D-COF-4.

## Results and Discussion

To testify the synthesis of crystalline frameworks involving a self-correction process, model reactions for the possible C=C bond exchange are firstly investigated *by* time-dependent in situ $^1$H-NMR spectroscopy at 95 °C, using *N,N*-dimethylformamide-$d_7$ (DMF-$d_7$) as solvent, $Cs_2CO_3$ as base, and 1,3,5-trimethoxybenzene as reference to calculate the yields (Figure S1). The model reaction of **M1** (1.0 equiv) and **M3** (1.0 equiv) generates **M2** and **M6**, indicating a C=C bond exchange process (Figure 2a): The $^1$H NMR peaks at ≈7.4, ≈7.7, and 2.4 ppm, assigned to the hydrogens (g, h, and f) of compound **M2** and hydrogen e and methyl group of **M6**, respectively, appeared within 5 mins. After a one-hour reaction time, **M6** and **M2** were obtained in ≈22 % yield according to the integration of peaks in NMR spectroscopy, with the ratio of ≈7:2 for **M1** (**M3**):**M6** (**M2**).

Based on the above NMR investigations, we propose two possible reaction pathways for converting compounds **M1** and **M3** into **M6** and **M2** (Figure 2b). Path I involve the retro-Knoevenagel reaction mechanism from compound **M1** to benzonitrile **M2** and benzaldehyde **M7**; afterwards, another Knoevenagel condensation between **M3** and **M7** would provide compound **M6**. Path II involves the Michael-addition of **M1** and **M3** forming the intermediate compound 1,3-dicyano-1,2-diphenyl-3-(*p*-tolyl)propan-1-ide (**M5**); the subsequent Michael-elimination of **M5** provides benzonitrile **M2** and compound **M6**.

To determine which reaction pathway is dominant for the conversion (C=C bond exchange) of compounds **M1** and **M3** into **M6** and **M2** under anhydrous conditions, the retro-Knoevenagel reaction of compound **M1** into **M2** and **M7** was also investigated at 95 °C, using DMF-$d_7$ as solvent, $Cs_2CO_3$ as base, and 1,3,5-trimethoxybenzene as reference to calculate the yields (Figure S2). The time-dependent $^1$H-NMR spectrum demonstrated that only the peaks of compound **M1** were identified without observing **M2** and **M7**. This result suggests that the proposed Path I can be excluded. To understand the Path II involving the Michael-addition-elimination mechanism, we particularly synthesized the Michael-addition product **M4** (R=H) according to the

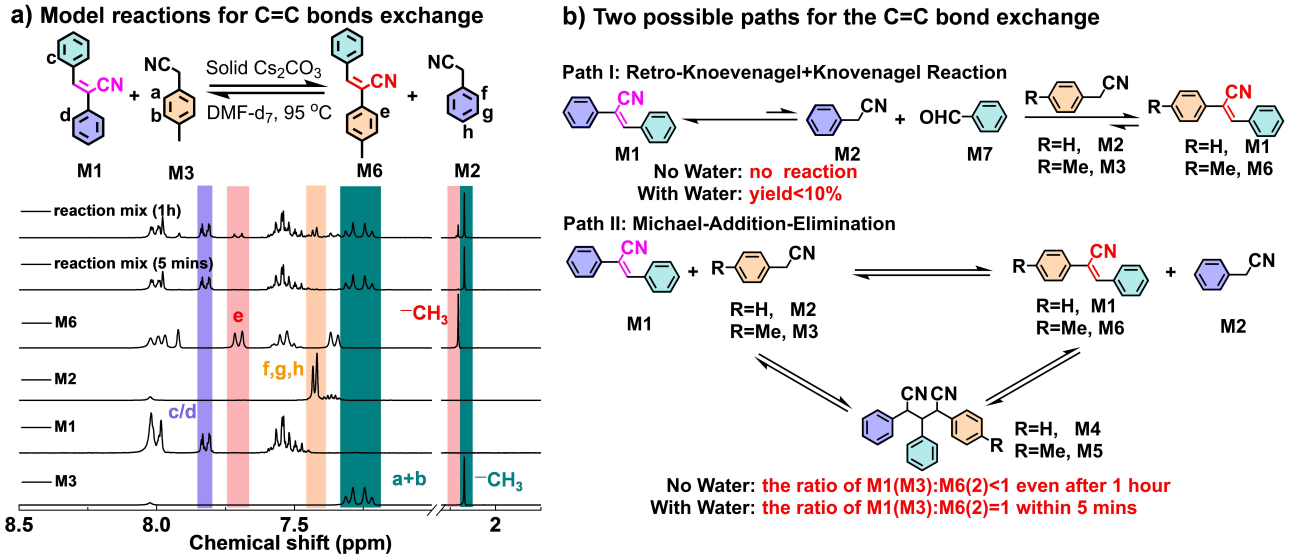


***Figure 2.*** a) Exploration of the possible C=C bond exchange via anhydrous $Cs_2CO_3$ catalyzed model reactions of **M1** and **M3** into **M6** and **M2** under anhydrous conditions with the in situ $^1$H-NMR study. b) The two possible routes for the C=C bond exchange from compounds **M3** and **M1** to **M6** and **M2**. Path I: Retro-Knoevenagel reaction from compound **M1** to **M2** and **M7**, plus an additional Knoevenagel condensation between benzaldehyde **M7** and **M3**, which would provide compound **M6**. Path II: Michael-addition from compounds **M3** and **M1** to the intermediate **M5**, followed by Michael-elimination from **M5** to **M6** and **M2**.


© 2022 The Authors. Angewandte Chemie International Edition published by Wiley-VCH GmbH

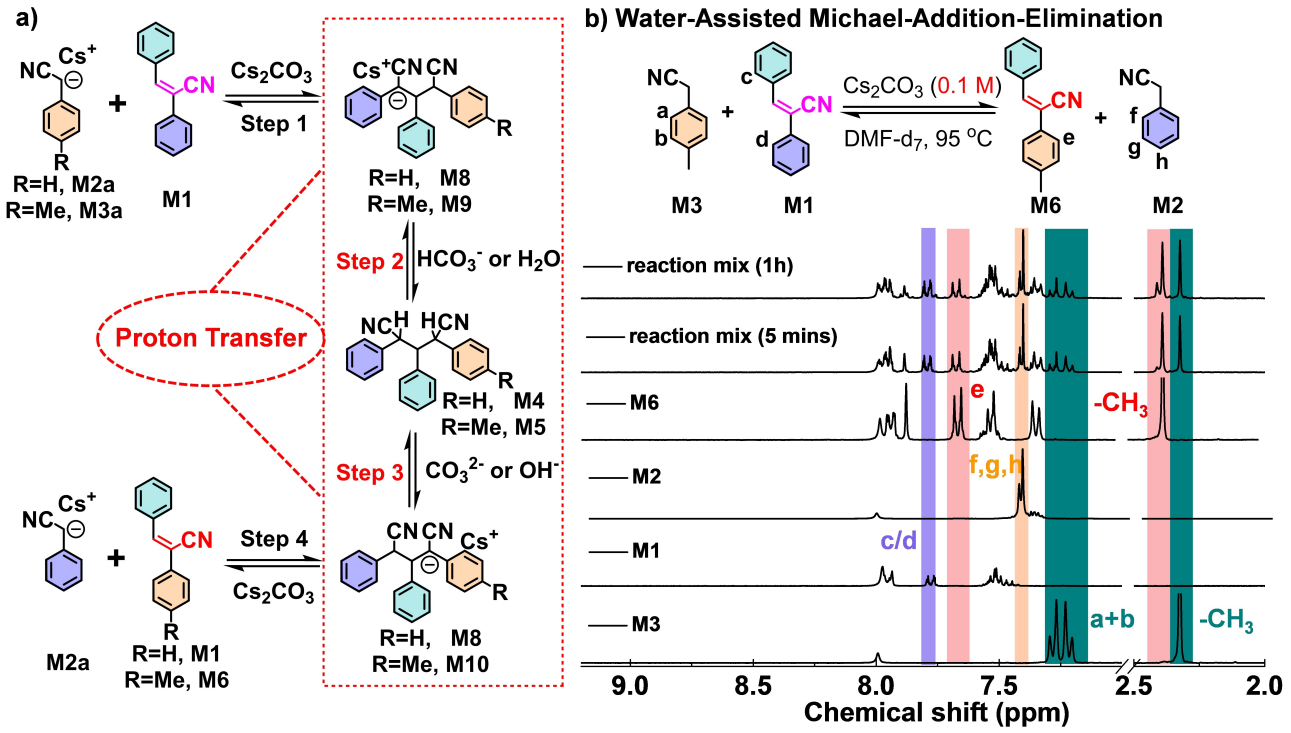


***Figure 3.*** a) Proposed mechanism for the Michael-addition-elimination reaction. b) $^{1}$H-NMR study of aqueous 0.1 M $Cs_2CO_3$ catalyzed substitution reaction between **M3** and **M1** for the C=C bond exchange.

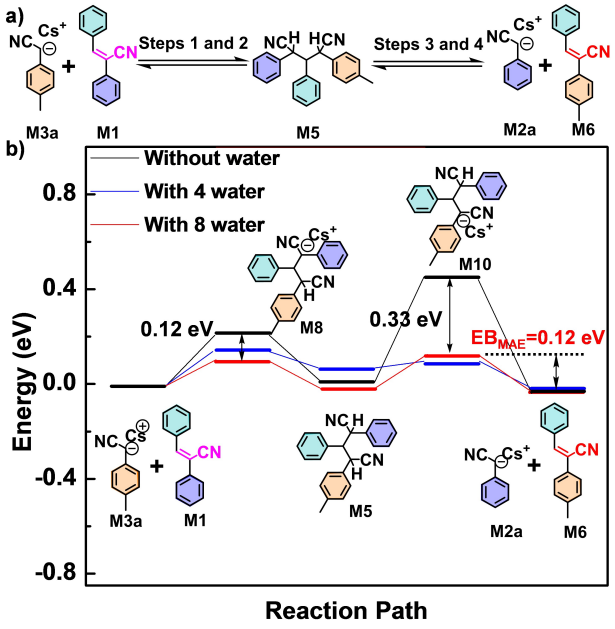


***Figure 4.*** a) The Michael-addition-elimination route from **M3a** and **M1** to **M2a** and **M6**. b) DFT calculation of Michael-addition-elimination reaction without water (black), with four water molecules (blue), and with eight water molecules (red).

reported literature (Figure S40–S42).[41] The Michael-elimination step was performed by subjecting compound **M4** at 95 °C, using DMF-$d_7$ as solvent, $Cs_2CO_3$ as base, and 1,3,5-trimethoxybenzene as reference to calculate the yields using in situ NMR investigation. Remarkably, after one-hour reaction, all $^{1}$H-NMR -peaks in the range of 3.5–5.5 ppm belonging to the aliphatic hydrogens i and j of **M4** (Figure 2b, R=H) disappeared (Figure S3). Instead, new NMR signals at ≈7.4 and ≈7.8 ppm were observed, which are assigned to the hydrogens (g, h, and f) in **M2** and hydrogens c or d in **M1** (R=H). The corresponding yield of compound **M2** and **M1** (Figure 2b, R=H) is estimated to be ≈95 %. Thereby, we can conclude that Path II (Michael-addition-elimination) is rational for the C=C bond exchange, which is distinguished from the hypothetical reversible Knoevenagel reaction for the first time.[42,43]

Encouraged by the above results, we further propose a four-step mechanism for the Michael-addition-elimination reaction *by* using $Cs_2CO_3$ as a catalyst (Figure 3a). The first two steps belong to the Michael-addition. In Step 1, the carbon anion specie **M3a** nucleophilic-ally attacks the CN-substituted vinylene linkage of compound **M1**, providing the intermediate anion **M9**. In Step 2, the intermediate **M9** is converted into the neutral intermediate **M5** via protonation. The next two steps deal with the Michael-elimination: In step 3, the deprotonation of **M5** yields anion specie **M10**. Then in step 4, **M10** dissociates into **M2a** and **M6**. Overall, the conversion is **M3a** + **M1** <=> **M2a** + **M6**.

In the proposed mechanism, both Steps 2 and 3 (Figure 3a) involve proton-transfer processes. Under $Cs_2CO_3$-catalyzed conditions, the $HCO_3^-$ and $CO_3^{2-}$ can be used as a donor/acceptor for the proton transfer. Consequently, the Michael-addition-elimination occurs in a slow rate due to the relevantly limited amount of proton. In this respect, we


© 2022 The Authors. Angewandte Chemie International Edition published by Wiley-VCH GmbH

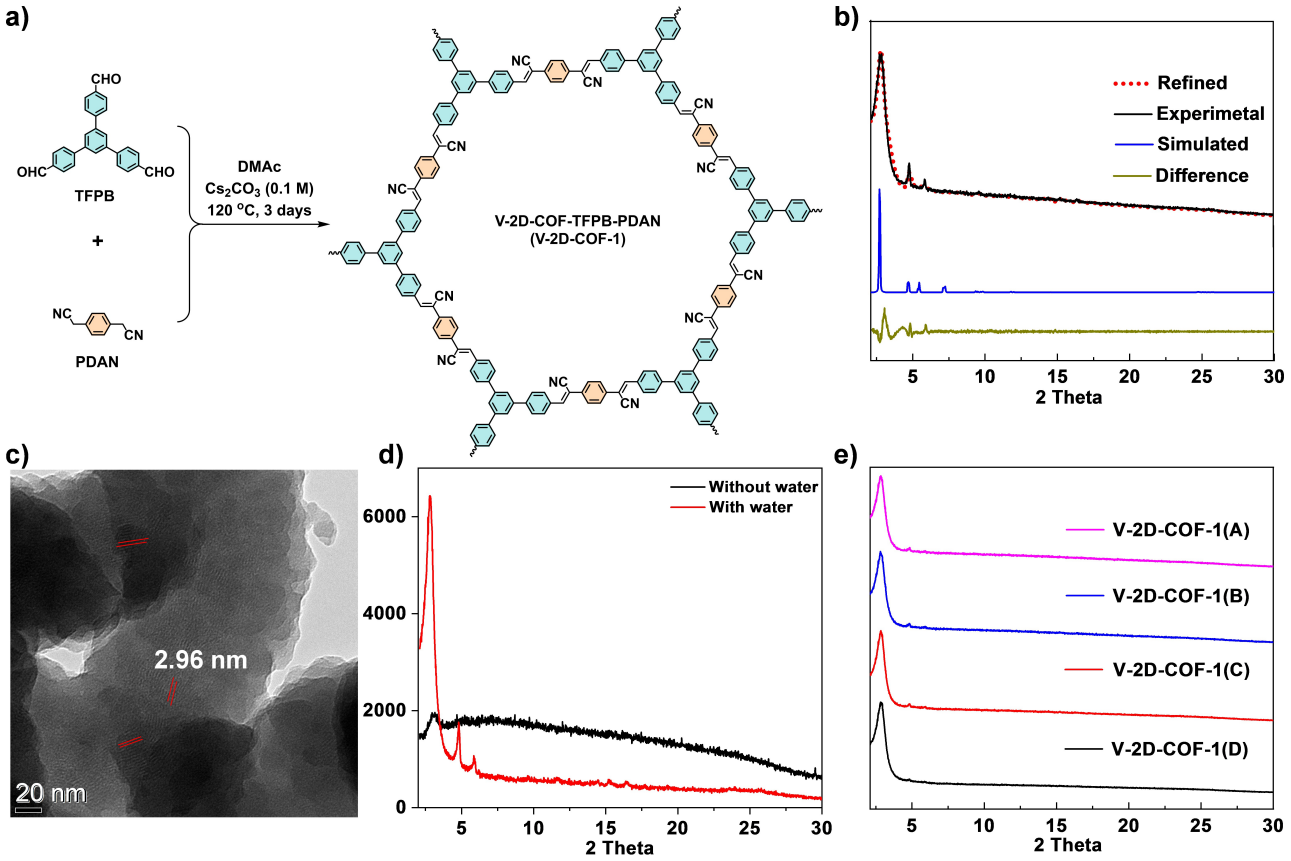


***Figure 5.*** a) The synthesis of V-2D-COF-1 via the water-assisted KMAE polymerization conditions. b) Corresponding experimental and simulated PXRD patterns of V-2D-COF-1. c) HR-TEM image of V-2D-COF-1 synthesized via water-assisted condition. d) The comparison of PXRD patterns of V-2D-COF-1 synthesized with and without the addition of water (measure parameters: step size: 1°, time: 60 s). e) The comparison of PXRD patterns of different V-2D-COF-1 batches synthesized via the water-assisted conditions.

assume that the Michael-addition-elimination for the C=C bond exchange can be mostly accelerated *by* the addition of small amount of water, which would generate sufficient $H_2O/OH^-$ as proton-donor/acceptor pair to replace the $HCO_3^-/CO_3^{2-}$ pair. It should be noted that the softness of $Cs^+$ makes $Cs_2CO_3$ rather soluble in organic solvents such as DMF and alcohol, which renders $Cs_2CO_3$ an excellent candidate base for studying the effect of water.[44,45]

To examine the influence of water on the Michael-addition-elimination, as shown in Figure 3b, the reaction between **M3** (1.0 equiv) and **M1** (1.0 equiv) was further studied by time-dependent in situ $^1$H-NMR at 95 °C with DMF-$d_7$ as the solvent and aqueous 0.1 M $Cs_2CO_3$ solution as the catalyst. Remarkably, the peaks at ≈7.8 (for **M1**) and ≈7.7 ppm (for **M6**) of the $^1$H-NMR spectrum suggested a ratio of 1:1 for **M1**:**M6** within 5 mins. Afterwards, the equilibrium was maintained (Figure S4). In contrast, the Michael-addition-elimination reaction with anhydrous condition presented a ratio of 7:2 for compounds **M1**:**M6** even after 1 h reaction time. This sharp contrast clearly demonstrates the crucial role of water in accelerating the C=C bond exchange. The Michael-elimination of intermediate **M4** was also investigated under the water-assisted condition, which resulted in compounds **M1** and **M2** with a yield of ≈92 % within 5 mins (Figure S6). It should be noted that the addition of water also enables the retro-Knoevenagel reaction of **M1** with a low yield for **M2** and **M7** (<10 %) in a one-hour reaction (Figure S7), which can additionally contribute to the efficiency of C=C bond exchange (Figure 2b).

To gain a deeper insight into the Michael-addition-elimination for the C=C bond exchange, DFT calculations were conducted to calculate the energy of each intermediate of the Knoevenagel condensation between **M2** and **M7** (Figure S8, S12–S14), and the Michael-addition-elimination between **M3** and **M1** (Figure 4a, Figure S9–S11) with zero, four and eight water molecules. For the Michael-addition-elimination, the intermediates of cesium 1,3-dicyano-2,3-diphenyl-1-(*p*-tolyl)propan-1-ide **M8** and **M10** possess the highest energy levels, which should determine the reaction rates. The energies of **M8** and **M10** are decreased by 0.12 and 0.33 eV with eight surrounding water molecules, compared to the corresponding ones without hydration (Figure 4b). This result further indicates that the addition of water can facilitate the Michael-addition-elimination reaction. It should be noted that the much lower energy barrier of the Michael-addition-elimination ($EB_{MAE}$ = 0.12 eV, Figure 4b) than the Knoevenagel ($EB_k$ = 0.43 eV, Figure S8) and retro-Knoevenagel ($EB_{rk}$ = 1.02 eV, Figure S8) reaction also suggests that the Michael-addition-elimination is the main driving force for the achieved C=C bonds exchange,


© 2022 The Authors. Angewandte Chemie International Edition published by Wiley-VCH GmbH

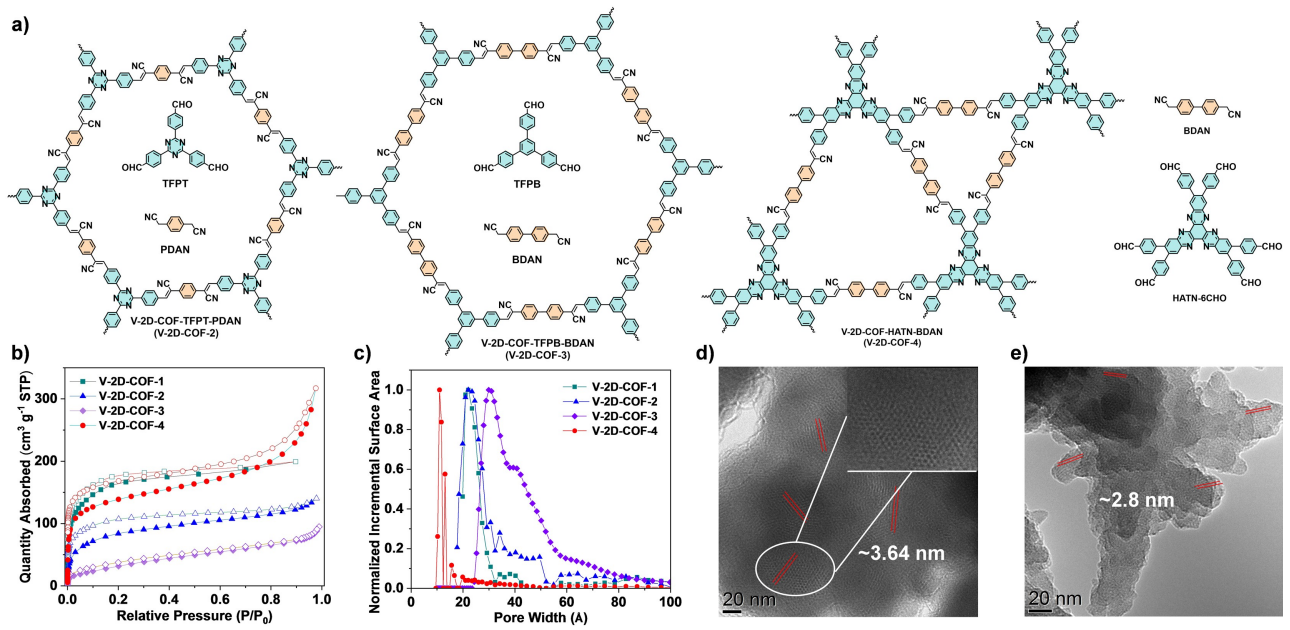


***Figure 6.*** a) The chemical structures of V-2D-COF-2, V-2D-COF-3, and V-2D-COF-4 that newly synthesized from several monomers, including TFPB, TFPT, HATN-6CHO, PDAN, and BDAN. b) $N_2$ adsorption–desorption isotherms and c) pore size distributions of V-2D-COFs synthesized via water-assisted KMAE polymerization conditions; HR-TEM images of d) V-2D-COF-3 and e) V-2D-COF-4, which are synthesized via water-assisted conditions.

which matches very well with above model reaction results (Figure 3b).

Encouraged by the dynamic covalent nature of the Michael-addition-elimination for the C=C bond exchange as described above, the combination of Knoevenagel polycondensation and water-assisted dynamic Michael-addition-elimination (classified as **KMAE** polymerization) was further demonstrated for the 2D polycondensation. The firstly reported CN-substituted V-2D-COF (V-2D-COF-1, Figure 5a)[24] can be synthesized by heating 1,3,5-tris-(4-fromylphenyl)benzene (TFPB, 1.0 equiv) and (1,4-phenylene)diacetonitrile (PDAN,1.5 equiv) in the mixture of *N,N*-dimethylacetamide (DMAc)/$Cs_2CO_3$ (0.1 M) at 120 °C for 3 days. After washing and drying, V-2D-COF-1 was obtained as yellowish powder in 80 % yield.

The simulated and experimental PXRD patterns as well as the difference plot confirmed the formation of crystalline frameworks (Figure 5b). Moreover, the high-resolution transmission electron microscopy (HR-TEM) study was carried out for V-2D-COF-1. The HR-TEM images revealed crystalline domains with periodic patterns of ≈2.96 nm, which matched well with the theoretical $d_{100}$-spacing value of ≈3.0 nm (Figure 5c). In contrast, the PXRD patterns of V-2D-COF-1 synthesized under strictly anhydrous reaction conditions showed much lower crystallinity (Figure 5d). Using the same PXRD parameters, the intensity of the (100) reflex (≈6000) of V-2D-COF-1 synthesized under water-assisted conditions is ≈3 times higher than the value (≈2000) of V-2D-COF-1 that was synthesized without the addition of water. The lower crystallinity of V-2D-COF-1 synthesized under the anhydrous condition can be explained by insufficient the error-correction process without involving the efficient C=C bond exchange. To reveal the reproducibility of the water-assisted condition, the synthesis of V-2D-COF-1 under aqueous 0.1 M $Cs_2CO_3$ catalyzed polymerization conditions were further conducted randomly five times. The PXRD patterns of all five batches from V-2D-COF-1 showed superior reproducibility (Figure 5e).

To demonstrate the versatility of the **KMAE** polymerization for the synthesis of various CN-substituted V-2D-COFs, another three examples of the CN-substituted V-2D-COFs (Figure 6a), including V-2D-COF-TFPT-PDAN (V-2D-COF-2), V-2D-COF-TFPB-BDAN (V-2D-COF-3), and V-2D-COF-HATN-BDAN (V-2D-COF-4) from different aromatic aldehydes [$C_3$-symmetric 1,3,5-tris-(4-fromylphenyl)benzene (TFPB), (2,4,6-tris(4-formylphenyl)-1,3,5-triazine (TFPT), 2,3,8,9,14,15-hexa(4-formylphenyl)-[2,3-a:2′,3′-c]phenazine (HATN-6CHO)) and aromatic nitrile [$C_2$-symmetric (1,4-phenylene)diacetonitrile (PDAN) and 2,2′-(biphenyl-4,4′-diyl)diacetonitrile (BDAN)] were also synthesized successfully under aqueous 0.1 M $Cs_2CO_3$ catalyzed conditions. Experimental and simulated PXRD patterns revealed that all four V-2D-COFs are highly crystalline. The detailed synthesis and characterization were described in the Supporting Information (Figure S15–S29).

$N_2$ adsorption-desorption measurements were performed to investigate the porosity of the above-mentioned V-2D-COFs. The BET surface areas of V-2D-COF-1, V-2D-COF-2, V-2D-COF-3, and V-2D-COF-4 are 603, 287, 127, and 504 $m^2 g^{-1}$, respectively (Figure 6b). Further nonlocal density functional theory (NLDFT) calculations reveal the pore size distributions of 2.3–3.2 nm for V-2D-COF-1 and V-2D-COF-2, 3.1–4.2 nm for V-2D-COF-3, ≈1.3 and ≈1.8 nm for dual-pore V-2D-COF-4 (Figure 6c). Notably, the surface


© 2022 The Authors. Angewandte Chemie International Edition published by Wiley-VCH GmbH

areas of V-2D-COF-1 ($602\,m^2\,g^{-1}$) and V-2D-COF-2 ($287\,m^2\,g^{-1}$) are higher than the values of corresponding reported V-2D-COFs synthesized via anhydrous $Cs_2CO_3$-catalyzed conditions (472, and $232\,m^2\,g^{-1}$).[24,38] It should be mentioned that these values are still lower than the theoretic surface areas ($\approx 2133.4\,m^2\,g^{-1}$ for V-2D-COF-1, $\approx 2013\,m^2\,g^{-1}$ for V-2D-COF-2, $\approx 2181.9\,m^2\,g^{-1}$ for V-2D-COF-3, $\approx 1376\,m^2\,g^{-1}$ for V-2D-COF-4). High-resolution transmission electron microscopy (HR-TEM) images of both V-2D-COF-3 (Figure 6d) and V-2D-COF-4 (Figure 6e) powder samples displayed polycrystalline structures, and the crystalline domain sizes range from 20 to 100 nm with periodic patterns of $\approx 3.64$, and $\approx 2.8$ nm, which matched well with the theoretical $d_{100}$-spacing values of 3.6, and 2.8 nm, respectively.

## Conclusion

In conclusion, we demonstrate a novel method for synthesizing highly crystalline V-2D-COFs via the combination of Knoevenagel polycondensation and water-assisted Michael-addition-elimination (KMAE polymerization). Through in situ high-temperature NMR measurements of model reactions and intermediate, the Michael-addition-elimination is clearly distinguished from the hypothetical reversible Knoevenagel reaction for the first time. Furthermore, the water-assisted Michael-addition-elimination is assigned as an efficient dynamic covalent chemistry for the direct C=C bond exchange, which endows the self-correction property to synthesize complicated extended structures. Indeed, DFT calculations indicate a reduced energy barrier of Michael-addition-elimination by the addition of water. The deep understanding of the reaction mechanism further guides the synthesis of four highly crystalline V-2D-COFs with crystalline domain sizes ranging from 20 to 100 nm. This work not only provides efficient dynamic C=C exchange chemistry for the synthesis of highly crystalline V-2D-COFs, but also pave the way for the future development of single crystalline V-2D-COFs and new type of vinylene-linked 2D-conjugated polymers for optoelectronic applications.

## Acknowledgements

We thank the financial support from the DFG for the CRC 1415 (No. 417590517), the ERC Consolidator Grant (T2DCP, NO. 819698), Coordination Networks: Building Blocks for Functional Systems (SPP 1928, COORNET), EU Graphene Flagship (GrapheneCore3; No. 881603), H2020-MSCA-ITN (ULTIMATE, No. 813036). We thank Dr. Petr Formanek (Leibniz Institute for Polymer Research, IPF, Dresden) for the TEM measurements. We thank Dr. Silvia Paasch (TU Dresden) for the solid $^{13}C$-NMR measurements. We also acknowledge the Center for Information Services and High-Performance Computing (ZIH) at TU Dresden for computational resources. MAA acknowledges the Materials Chemistry Consortium for HPC time on YOUNG (EP/T022213). Open Access funding enabled and organized by Projekt DEAL.

## Conflict of Interest

The authors declare no conflict of interest.

## Data Availability Statement

The data that support the findings of this study are available in the supplementary material of this article.

**Keywords:** Dynamic Chemistry · Knoevenagel Polymerization · Two-Dimensional Organic Framework · Vinylene-Linked Systems

[1] P. J. Waller, F. Gándara, O. M. Yaghi, *Acc. Chem. Res.* **2015**, *48*, 3053–3063.
[2] N. Huang, P. Wang, D. Jiang, *Nat. Rev. Mater.* **2016**, *1*, 16068.
[3] M. Bieri, M. Treier, J. Cai, K. Aït-Mansour, P. Ruffieux, O. Gröning, P. Gröning, M. Kastler, R. Rieger, X. Feng, K. Müllen, R. Fasel, *Chem. Commun.* **2009**, 6919–6921.
[4] Y. Jin, Y. Hu, W. Zhang, *Nat. Chem. Rev.* **2017**, *1*, 0056.
[5] S. Kandambeth, K. Dey, R. Banerjee, *J. Am. Chem. Soc.* **2019**, *141*, 1807–1822.
[6] J. Mahmood, M. A. R. Anjum, J. B. Baek, *Adv. Mater.* **2019**, *31*, 1805062.
[7] R. R. Liang, S. Y. Jiang, R.-H. A, X. Zhao, *Chem. Soc. Rev.* **2020**, *49*, 3920–3951.
[8] M. Yu, R. Dong, X. Feng, *J. Am. Chem. Soc.* **2020**, *142*, 12903–12915.
[9] K. Geng, T. He, R. Liu, S. Dalapati, K. T. Tan, Z. Li, S. Tao, Y. Gong, Q. Jiang, D. Jiang, *Chem. Rev.* **2020**, *120*, 8814–8933.
[10] W. Liu, K. P. Loh, *Acc. Chem. Res.* **2017**, *50*, 522–526.
[11] R. Dong, P. Han, H. Arora, M. Ballabio, M. Karakus, Z. Zhang, C. Shekhar, P. Adler, P. S. Petkov, A. Erbe, S. C. B. Mannsfeld, C. Felser, T. Heine, M. Bonn, X. Feng, E. Cánovas, *Nat. Mater.* **2018**, *17*, 1027–1032.
[12] S. Wan, F. Gándara, A. Asano, H. Furukawa, A. Saeki, S. K. Dey, L. Liao, M. W. Ambrogio, Y. Y. Botros, X. Duan, S. Seki, J. F. Stoddart, O. M. Yaghi, *Chem. Mater.* **2011**, *23*, 4094–4097.
[13] J. Guo, Y. Xu, S. Jin, L. Chen, T. Kaji, Y. Honsho, M. A. Addicoat, J. Kim, A. Saeki, H. Ihee, S. Seki, S. Irle, M. Hiramoto, J. Gao, D. Jiang, *Nat. Commun.* **2013**, *4*, 2736.
[14] N. Huang, K. H. Lee, Y. Yue, X. Xu, S. Irle, Q. Jiang, D. Jiang, *Angew. Chem. Int. Ed.* **2020**, *59*, 16587–16593; *Angew. Chem.* **2020**, *132*, 16730–16736.
[15] K. Sakaushi, M. Antonietti, *Acc. Chem. Res.* **2015**, *48*, 1591–1600.
[16] P. Kuhn, M. Antonietti, A. Thomas, *Angew. Chem. Int. Ed.* **2008**, *47*, 3450–3453; *Angew. Chem.* **2008**, *120*, 3499–3502.
[17] K. Wang, L. M. Yang, X. Wang, L. Guo, G. Cheng, C. Zhang, S. Jin, B. Tan, A. Cooper, *Angew. Chem. Int. Ed.* **2017**, *56*, 14149–14153; *Angew. Chem.* **2017**, *129*, 14337–14341.
[18] M. R. Rao, Y. Fang, S. De Feyter, D. F. Perepichka, *J. Am. Chem. Soc.* **2017**, *139*, 2421–2427.
[19] D. L. Pastoetter, S. Xu, M. Borrelli, M. Addicoat, B. P. Biswal, S. Paasch, A. Dianat, H. Thomas, R. Berger, S. Reineke, E. Brunner, G. Cuniberti, M. Richter, X. Feng, *Angew. Chem. Int. Ed.* **2020**, *59*, 23620–23625; *Angew. Chem.* **2020**, *132*, 23827–23832.


© 2022 The Authors. Angewandte Chemie International Edition published by Wiley-VCH GmbH

[20] S. Xu, H. Sun, M. Addicoat, B. P. Biswal, F. He, S. W. Park, S. Paasch, T. Zhang, W. Sheng, E. Brunner, Y. Hou, M. Richter, X. Feng, *Adv. Mater.* **2021**, *33*, 2006274.
[21] G. Zhang, Z. A. Lan, X. Wang, *Angew. Chem. Int. Ed.* **2016**, *55*, 15712–15727; *Angew. Chem.* **2016**, *128*, 15940–15956.
[22] P. Pachfule, A. Acharjya, J. Roeser, T. Langenhahn, M. Schwarze, R. Schomäcker, A. Thomas, J. Schmidt, *J. Am. Chem. Soc.* **2018**, *140*, 1423–1427.
[23] S. Xu, G. Wang, B. P. Biswal, M. Addicoat, S. Paasch, W. Sheng, X. Zhuang, E. Brunner, T. Heine, R. Berger, X. Feng, *Angew. Chem. Int. Ed.* **2019**, *58*, 849–853; *Angew. Chem.* **2019**, *131*, 859–863.
[24] X. Zhuang, W. Zhao, F. Zhang, Y. Cao, F. Liu, S. Bi, X. Feng, *Polym. Chem.* **2016**, *7*, 4176–4181.
[25] E. Jin, M. Asada, Q. Xu, S. Dalapati, M. A. Addicoat, M. A. Brady, H. Xu, T. Nakamura, T. Heine, Q. Chen, D. Jiang, *Science* **2017**, *357*, 673–676.
[26] T. He, K. Geng, D. Jiang, *Trends Chem.* **2021**, *3*, 431–444.
[27] S. Xu, M. Richter, X. Feng, *Acc. Mater. Res.* **2021**, *2*, 252–265.
[28] X. Li, *Mater. Chem. Front.* **2021**, *5*, 2931–2949.
[29] H. Lyu, C. S. Diercks, C. Zhu, O. M. Yaghi, *J. Am. Chem. Soc.* **2019**, *141*, 6848–6852.
[30] S. Bi, C. Yang, W. Zhang, J. Xu, L. Liu, D. Wu, X. Wang, Y. Han, Q. Liang, F. Zhang, *Nat. Commun.* **2019**, *10*, 2467.
[31] S. Bi, P. Thiruvengadam, S. Wei, W. Zhang, F. Zhang, L. Gao, J. Xu, D. Wu, J. S. Chen, F. Zhang, *J. Am. Chem. Soc.* **2020**, *142*, 11893–11900.
[32] Z. Wang, Y. Yang, Z. Zhao, P. Zhang, Y. Zhang, J. Liu, S. Ma, P. Cheng, Y. Chen, Z. Zhang, *Nat. Commun.* **2021**, *12*, 1982.
[33] S. Xu, Y. Li, B. P. Biswal, M. A. Addicoat, S. Paasch, P. Imbrasas, S. W. Park, H. Shi, E. Brunner, M. Richter, S. Lenk, S. Reineke, X. Feng, *Chem. Mater.* **2020**, *32*, 7985–7991.
[34] E. Jin, J. Li, K. Geng, Q. Jiang, H. Xu, Q. Xu, D. Jiang, *Nat. Commun.* **2018**, *9*, 4143.
[35] W. R. Cui, C. R. Zhang, W. Jiang, F. F. Li, R. P. Liang, J. Liu, J. D. Qiu, *Nat. Commun.* **2020**, *11*, 436.
[36] S. Li, L. Li, Y. Li, L. Dai, C. Liu, Y. Liu, J. Li, J. Lv, P. Li, B. Wang, *ACS Catal.* **2020**, *10*, 8717–8726.
[37] E. Jin, Z. Lan, Q. Jiang, K. Geng, G. Li, X. Wang, D. Jiang, *Chem* **2019**, *5*, 1632–1647.
[38] Y. Zhao, H. Liu, C. Wu, Z. Zhang, Q. Pan, F. Hu, R. Wang, P. Li, X. Huang, Z. Li, *Angew. Chem. Int. Ed.* **2019**, *58*, 5376–5381; *Angew. Chem.* **2019**, *131*, 5430–5435.
[39] R. Bu, L. Zhang, X. Y. Liu, S. L. Yang, G. Li, E. Q. Gao, *ACS Appl. Mater. Interfaces* **2021**, *13*, 26431–26440.
[40] M. Yang, C. Mo, L. Fang, J. Li, Z. Yuan, Z. Chen, Q. Jiang, X. Chen, D. Yu, *Adv. Funct. Mater.* **2020**, *30*, 2000516.
[41] S. Shimizu, S. Shirakawa, T. Suzuki, Y. Sasaki, *Tetrahedron* **2001**, *57*, 6169–6173.
[42] C. Jiao, L. Gao, H. Zhang, B. Yu, H. Cong, Y. Shen, *Biomacromolecules* **2020**, *21*, 1234–1242.
[43] N. F. König, D. Mutruc, S. Hecht, *J. Am. Chem. Soc.* **2021**, *143*, 9162–9168.
[44] R. Rabie, M. M. Hammouda, K. M. Elattar, *Res. Chem. Intermed.* **2017**, *43*, 1979–2015.
[45] Y. P. Patil, P. J. Tambade, S. R. Jagtap, B. M. Bhanage, *Green Chem. Lett. Rev.* **2008**, *1*, 127–132.

Manuscript received: February 15, 2022
Accepted manuscript online: March 6, 2022
Version of record online: March 21, 2022


© 2022 The Authors. Angewandte Chemie International Edition published by Wiley-VCH GmbH